Acknowledgment. This research was supported by the Natural Sciences and Engineering Research Council of Canada, in the form of an operating grant to Y.K. and a University Undergraduate Student Research Award to W.W.Y.S. T.Y.H.W. thanks the governments of Canada and British Columbia for the Award of Challenge 89.

FEATURE ARTICLE

Microemulsions: A Qualitative Thermodynamic Approach

M. Kahlweit,* R. Strey, and G. Busse

Max-Planck-Institut für biophysikalische Chemie, Postfach 2841, D 3400 Göttingen, F.R.G.
(Received: October 25, 1989)

Microemulsions, that is, stable colloidal dispersions of water and nonpolar solvents stabilized by amphiphiles, are of growing interest in research and industry. The phase behavior of the multicomponent mixture is essentially determined by the features of corresponding binary mixtures. The efficiency of an amphiphile in solubilizing the solvents reaches its maximum in the temperature interval in which the mixture separates into three coexisting liquid phases. The domain size of the dispersion is determined by the interfacial tension between the aqueous and the oil-rich phase in the presence of a saturated monolayer. Because the interfacial tension reaches its minimum in the three-phase interval and, furthermore, decreases with increasing amphiphilicity, the transition from weakly structured solutions to microemulsions is gradual. It is, therefore, suggested that microemulsions be defined as stable colloidal dispersions of domains sufficiently large for the dispersed solvent to exhibit the properties as, e.g., the dielectric number of a bulk phase.

I. Introduction

This paper deals with liquid mixtures of water (A), nonpolar solvents (oils) (B), nonionic (C) or ionic amphiphiles (D), and salts (E). The mutual solubility between water and oils is very low. However, if an amphiphile is added, the mutual solubility increases until, at a sufficiently high amphiphile concentration, the mixture becomes homogeneous. As experiment shows, the distribution of the amphiphiles between the aqueous and the oil-rich phase changes with temperature: at ambient temperatures, nonionic amphiphiles are more soluble in the (lower) aqueous phase (Winsor I, in this paper denoted by $\underline{2}$), at elevated temperatures they are more soluble in the (upper) oil-rich phase (Winsor II, denoted by $\bar{2}$), whereas with ionic amphiphiles the reverse is true. Within a well-defined temperature interval ΔT in between, however, the mixture may separate into three coexisting liquid phases, a (lower) water-rich (a), a (middle) amphiphile-rich (c), and an (upper) oil-rich phase (b) (Winsor III, denoted by 3). Close to the mean temperature $\bar{T}$ of ΔT one finds the highest efficiency of the amphiphile with respect to homogenizing equal masses of water and oil, and a minimum of the interfacial tension between phase a and b. This review compiles some facts about these mixtures which may serve as a basis for applying them in research and industry, as well as for further theoretical work. The paper is divided into three parts: in the first part (section II) it is shown that the separation into three coexisting liquid phases, the maximum of the mutual solubility between water and oil, and the minimum of the interfacial tension between phase a and b near $\bar{T}$ are inevitable consequences of the laws of thermodynamics irrespective of the nature of the components, and are thus not particular properties of microemulsions. In the second part (sections III–VI) it is demonstrated that the mean temperature $\bar{T}$ of the three-phase interval ΔT is essentially determined by the critical temperatures of the binary B–C (or D) and A–C (or D) mixtures. In the third part, finally, the essential difference between microemulsions and weakly structured multicomponent liquid mixtures is discussed.

Some of the results are represented in schematic figures. They are, however, substantiated by many experiments performed by various groups in North America, Europe, Japan, and Australia.

II. General Considerations

In the absence of external fields, in particular, at zero gravity, a ternary mixture has four independent thermodynamic variables, namely the temperature T, the external pressure p, and two composition variables the choice of which is a matter of convenience. Because experiment shows that the effect of pressure is weak compared with that of temperature, one may dispense with p by keeping it constant. The phase behavior of a ternary mixture can then be represented exactly in an upright phase prism with the Gibbs triangle A–B–C (or D) as the base and T as the ordinate as shown in Figure 1. If not otherwise stated, we choose as composition variables the mass fraction of the oil in the mixture of water and oil

$$\alpha \equiv B/(A + B) \tag{II.1}$$

and that of the amphiphile in the mixture of all three components

$$\gamma \equiv C/(A + B + C) \tag{II.2}$$

both expressed in weight percent. At constant pressure, each point in the phase prism is then unambiguously defined by a set of T, α, and γ.

Consider first the origin of the separation of a ternary mixture into three coexisting condensed phases. As has been clarified in the beginning of this century,[1] it arises from the interplay between the miscibility gaps of the corresponding three binary mixtures representing the sides of the phase prism. If each of the binary mixtures shows a miscibility gap near the temperature of ex-

(1) Schreinemakers, F. A. H. In *Die heterogenen Gleichgewichte*; Rooze-boom, H. W., Ed.; Vieweg: Braunschweig, 1913; Vol. III/2. For a more recently published textbook in English see: Prince, A. *Alloy Phase Equilibria*; Elsevier: Amsterdam, 1966.

0022-3654/90/2094-3881$02.50/0

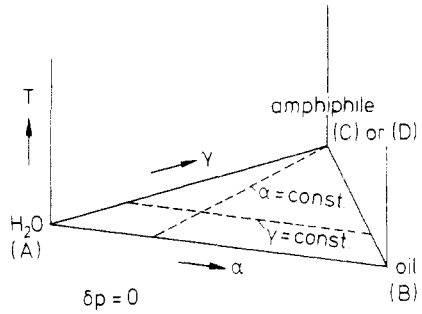

Figure 1. The phase prism with the Gibbs triangle A–B–C (or D) as the base, and T as the ordinate.

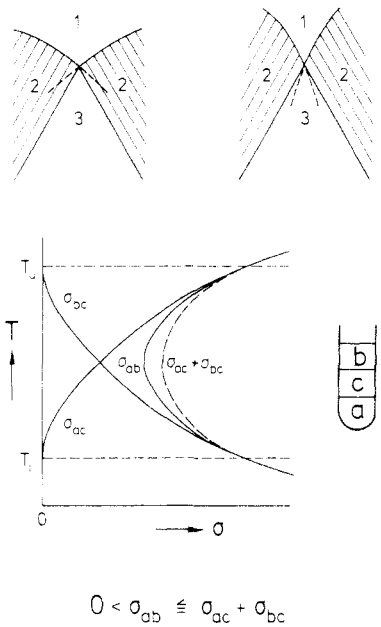

Figure 2. (Top) Phase boundaries in the c corner of the three-phase triangle. (Bottom) Interfacial tensions between the three phases vs T (schematic).

periment, these will extend into the phase prism where they interact with each other. In case of a sufficiently strong interaction, this gives rise to isothermal three-phase triangles within the prism. As Meijering showed in 1950,[2] even the simplest conceivable model for a nonideal ternary mixture, namely a regular mixture, separates into three phases if the parameters appearing in the excess free energy are appropriately chosen. In 1949, Tompa[3] had already studied three-phase equilibria in ternary mixtures with polymers as one of the components, applying the Flory–Huggins model. The separation of a ternary mixture into three coexisting condensed phases is thus not a particular property of mixtures of water, oil, and amphiphile, but can also be found in mixtures without amphiphiles, e.g., in ternary metallic alloys.

Consider now the origin of the maximum of the mutual solubility between water and oil near the mean temperature of the three-phase body. The isothermal three-phase triangles are surrounded by three two-phase regions. As can be seen in Figure 4, the intersections of the boundaries of these two-phase regions shape a shallow groove at the corners of the three-phase triangle. As Schreinemakers[4] showed in 1913, these grooves are a consequence of the thermodynamic stability conditions that require the boundaries between the homogeneous and the two-phase regions to intersect at each corner of the three-phase triangle such that both their extensions pass either into the adjacent two-phase region, or both into the triangle (Figure 2, top). As a consequence, the homogeneous region next to the c corner cuts a groove into the

(2) Meijering, J. L. *Philips Res. Rep.* **1950**, *5*, 333; **1951**, *6*, 183.
(3) Tompa, H. *Trans. Faraday Soc.* **1949**, *45*, 1142.
(4) Reference 1, p 17. See also: Wheeler, J. C. *J. Chem. Phys.* **1974**, *61*, 4474.

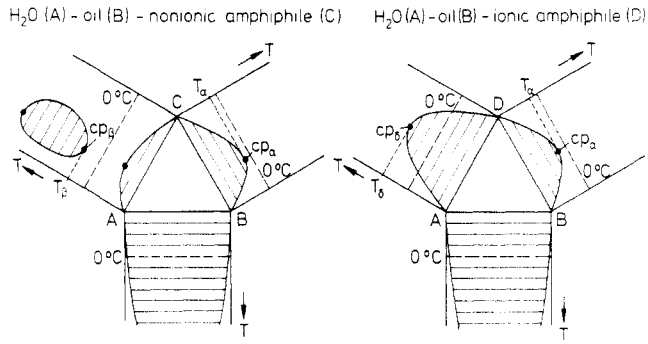

Figure 3. Unfolded phase prisms showing the phase diagrams of the binary mixtures (schematic).

body of heterogeneous phases which is the reason for the enhanced mutual solubility between component A and B in phase c. In weakly structured mixtures, the extensions pass, in general, into the adjacent two-phase regions so that the groove is rather shallow. In mixtures with medium- and long-chain amphiphiles as component C, however, the extensions pass into the three-phase triangle so that the groove is rather deep, its depth increasing with increasing efficiency of the amphiphile.

Consider, finally, the origin of the minimum of the interfacial tension σ_{ab} between the water-rich (a) and the oil-rich phase (b). As is shown in Figure 4, the three-phase triangle in mixtures with nonionic amphiphiles appears at the (lower) temperature T_l by separation of the aqueous phase into phases a and c at a plait point on the water-rich end point of the (lower) critical tie line of the three-phase body. With rising temperature, phase c moves clockwise (if looked at from above) on an ascending curve around the binodal surface to the oil-rich side where it merges with phase b at the (upper) temperature T_u at a plait point on the oil-rich end point of the (upper) critical tie line of the three-phase body. Because phases a and c separate at a plait point, the interfacial tension σ_{ac} between these two phases must rise from zero (at T_l) to increase monotonically with rising temperature (Figure 2, bottom). Because, on the other hand, phases c and b merge at a plait point, the interfacial tension σ_{bc} between these two phases must decrease monotonically with rising temperature to vanish at T_u. Thermodynamic stability requires

$$0 < \sigma_{ab} \leq \sigma_{ac} + \sigma_{bc} \qquad \text{(II.3)}$$

Because σ_{ac} and σ_{bc} are monotonic functions with reverse temperature dependence, σ_{ab} must show a minimum close to the mean temperature

$$\bar{T} = (T_l + T_u)/2 \qquad \text{(II.4)}$$

of the three-phase temperature interval

$$\Delta T \equiv T_u - T_l \qquad \text{(II.5)}$$

The minimum of σ_{ab} close to $\bar{T}$ is thus the consequence of the nearness of two critical end points. Actually, experiment shows that, in mixtures with medium- and long-chain amphiphiles, the inequality in eq II.3

$$0 < \sigma_{ab} < \sigma_{ac} + \sigma_{bc} \qquad \text{(II.6)}$$

holds as indicated by the full σ_{ab} curve in Figure 2. If the effect of gravity is reduced by removing the middle phase (c) until only a drop of it is left, the drop does not spread across the water/oil interface but contracts to a lens floating on that interface.

III. The Binary Phase Diagrams

In sections III–VI it will be shown that the position of the three-phase body within the phase prism, expressed in terms of its mean temperature $\bar{T}$, is essentially determined by the critical temperatures of the miscibility gaps in the two binary mixtures B–C (or D), and A–C (or D). For discussing the properties of the three binary phase diagrams A–B, B–C (or D), and A–C (or D), it is convenient to unfold the phase prisms of the ternary mixtures as shown in Figure 3. Each of the binary diagrams

shows, for thermodynamic reasons, a (lower) miscibility gap with an upper critical point the coordinates of which depend on the outcome of the competition between the interaction energies between the molecules and entropy. The phase diagrams of water–oil mixtures are, evidently, independent of the nature of the amphiphile. The critical points of their miscibility gaps lie well above the boiling points of the mixtures and play no role in the further discussion. Accordingly, the low mutual solubility between the two can be considered as being independent of temperature. The phase diagrams of oil–amphiphile mixtures are quite similar for nonionic and ionic amphiphiles. Their critical points (cp_α) lie close to the melting points of the mixtures. For a given amphiphile, the composition of cp_α moves toward the amphiphile-rich side with increasing carbon number, that is, increasing molar volume of the oil.[5] The critical temperature T_α rises with increasing carbon number of the oil (for a given amphiphile) but drops with increasing carbon number of the tail of the amphiphile (for given head group and given oil).

The major difference between nonionic and ionic amphiphiles exhibits itself in the phase diagrams of the water–amphiphile mixtures. Consider first single-tailed nonionic amphiphiles. The hydrophobic interaction between their head groups and water makes their lower miscibility gap lie, in general, below the melting point. At ambient temperatures, water and nonionic amphiphiles are thus completely miscible. With rising temperature, however, water becomes an increasingly poorer solvent for nonionic amphiphiles, which makes the miscibility gap reappear at elevated temperatures at a lower critical point (cp_β) that plays an important role in the phase behavior of ternary A–B–C mixtures. This upper gap is, again for thermodynamic reasons, a "closed loop". For a given head group, the composition of cp_β moves toward the water-rich side with increasing carbon number of the tail. The critical temperature T_β rises with increasing hydrophilicity of the head (for a given tail) but drops with increasing carbon number of the tail (for a given head).[6] The upper critical points of the loops lie, in general, above the boiling point and play no role in further discussion.

Ionic amphiphiles, on the other hand, do not show such an upper loop. On the contrary, as one raises temperature, water becomes an increasingly better solvent for ionic amphiphiles due to the increasing dissociation of the head groups and thus increasing hydrophilic interaction. In mixtures with ionic amphiphiles, it is thus the upper critical piont cp_δ of the (lower) A–D gap that plays an important role in the phase behavior of A–B–D mixtures. Being an upper critical point, its critical temperature T_δ drops with increasing hydration energy of the head (for a given tail) but rises with increasing carbon number of the tail (for a given head). With standard single-tailed ionics as, e.g., SDS, T_δ appears to lie well below the melting point, whereas with double-tailed ionics, T_δ varies between temperatures near the melting point (AOT) and above the boiling point (Texas I).

Summarized, increasing attractive hydrophilic interaction between the amphiphiles and water makes T_β rise but T_δ drop, whereas increasing repulsive hydrophobic interaction makes T_β drop but T_δ rise. When the interaction energies between water and nonionic or ionic amphiphiles are modeled, their temperature dependence must be such that for nonionics water is a better solvent than oil at ambient temperatures, but a poorer solvent at elevated temperatures. This makes the critical line change from the oil-rich to the water-rich side with rising temperature. For ionic amphiphiles, on the other hand, the temperature dependence must be such that water is a poorer solvent than oil at low temperatures, but a better one at elevated temperatures so that the critical line changes from the water-rich to the oil-rich side with rising temperature.

In fact the binary phase diagrams, in particular, of water–amphiphile mixtures are much more complicated. The competition between hydrophilic and hydrophobic interactions between amphiphiles and solvents leads to a preferential adsorption of amphiphiles at interfaces between water and nonpolar phases, to the formation of association colloids (micelles), and, at higher amphiphile concentrations, to the formation of lyotropic mesophases (liquid crystals). As for predicting the position of the three-phase bodies on the temperature scale, however, it suffices to study the dependence of the critical temperatures T_α, T_β, and T_δ of the binary miscibility gaps on the chemical nature of the components. This, furthermore, permits predicting the effect of additives like salts by studying their effect on the phase diagram of each binary mixture.

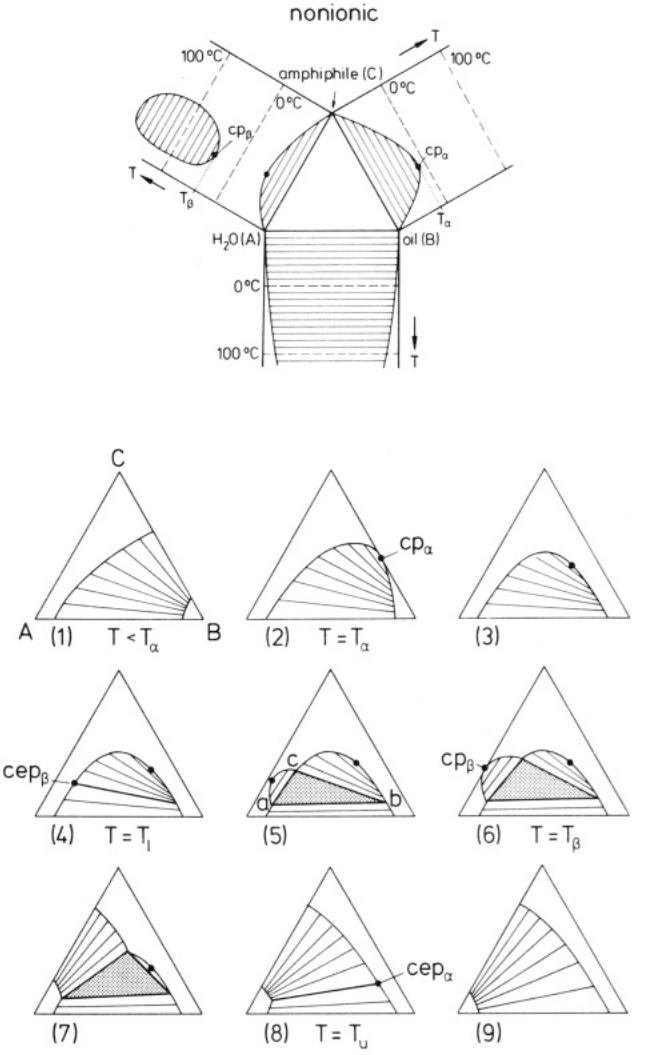

Figure 4. Evolution of the three-phase triangle with rising temperature in a mixture with a nonionic amphiphile (schematic).

IV. Evolution of the Three-Phase Body

The evolution of the three-phase body in mixtures with nonionic and ionic amphiphiles is analogous, except for being reverse with respect to temperature. It, therefore, suffices to discuss the evolution of the three-phase body within the phase prism in mixtures with nonionic amphiphiles. Figure 4 shows on top again the unfolded phase prism for an A–B–C mixture. Consider now the evolution of isothermal sections through the phase prism with rising temperature. At temperatures below T_α, both the A–B and the B–C mixtures show a miscibility gap, whereas the A–C mixture is completely miscible. Accordingly, an isothermal section through the phase prism shows a connected miscibility gap that extends from the A–B to the B–C side of the Gibbs triangle (upper left). At T_α, this gap disconnects from the B–C side of the Gibbs triangle at cp_α. With further rising temperature, the plait point first remains on the oil-rich side, lying on a critical line cl_α that enters the phase prism at cp_α and ascends into the prism (upper right).

(5) See Figure 6 in: Kahlweit, M.; Strey, R. *Angew. Chem., Int. Ed. Engl.* **1985**, *24*, 654.
(6) See Figure 6 in: Kahlweit, M.; Strey, R.; Haase, D.; Firman, P. *Langmuir* **1988**, *4*, 785.

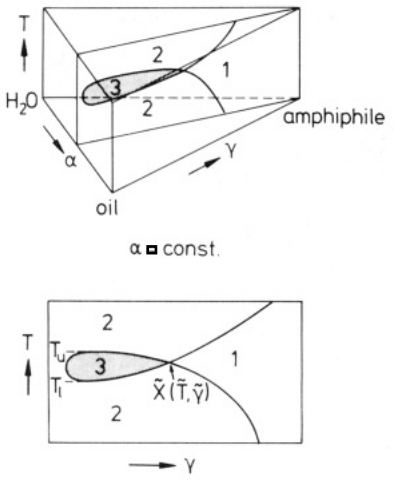

Figure 5. Vertical section through the phase prism at constant α (top), yielding a pseudobinary phase diagram with section through the three-phase body, and locus $\tilde{X}$ of amphiphile-rich phase (bottom, both schematic).

As one approaches the lower critical point cp_β of the A–C loop, the critical line cl_β that enters the phase prism at cp_β will eventually collide with the "central" miscibility gap. Whether cl_β ascends or descends into the prism, plays no role in this discussion. On Figure 4 it is assumed that cl_β descends into the prism. Accordingly, it appears at T_l as second plait point on the water-rich side of the central miscibility gap (center left). Thermodynamics requires that this makes the aqueous phase separate into a water-rich (a) and an amphiphile-rich phase (c), so that the tie line with the critical end point cep_β (on its water-rich side) represents the lower critical tie line of the three-phase body. As one raises T further, the upper A–C loops grow. Consequently, phase a moves toward the A corner, whereas phase c moves along an ascending trajectory around the binodal surface toward the oil-rich side of the Gibbs triangle to merge with phase b at T_u, so that the tie line with the critical end point cep_α (on its oil-rich side) represents the upper critical tie line of the three-phase body (bottom center). At temperatures above T_u, isothermal sections, accordingly, show a connected miscibility gap that extends from the A–B to the A–C side of the Gibbs triangle (bottom right).

With ionic amphiphiles one finds the reverse evolution. At low temperatures, the plait point of the central miscibility gap lies on the water-rich side. As one raises the temperature, the oil-rich phase separates at T_l into an oil-rich (b) and an amphiphile-rich phase (c), the end point of the descending critical line cl_α defining the lower critical tie line. With further rising temperature, phase b moves toward the B corner, whereas phase c moves on an ascending curve around the binodal surface to the water-rich side to merge with phase a at T_u at the end point of the critical line cl_δ that enters the phase prism at cp_δ, and defines the position of the upper critical tie line of the three-phase body.

A convenient procedure for determining the position and extensions of the three-phase bodies is to erect vertical sections through the phase prisms at $\alpha = 50$ wt % by mixing equal masses of water and oil and then adding various amounts of the amphiphile and observing the number of phases at fixed γ with rising temperature. This yields pseudobinary phase diagrams as shown schematically on bottom of Figure 5. At a sufficiently high γ, one finds a homogeneous mixture between melting and boiling point, at a somewhat lower γ, the phase sequence $2 \rightarrow 1 \rightarrow 2$, t a even lower γ, the sequence $2 \rightarrow 3 \rightarrow 2$, and at very low γ two phases between melting and boiling point. The minimum of the lower boundary of the section through the three-phase body gives T_l, the maximum of the upper boundary T_u, whereas the amphiphile concentration $\tilde{\gamma}$ at point $\tilde{X}$ represents a measure for the efficiency of the amphiphile, namely the minimum amount of amphiphile required for completely homogenizing equal masses of water and oil. Point $\tilde{X}$ is unambiguously defined by $\tilde{\gamma}$ and its temperature $\tilde{T}$, which lies close to the mean temperature $\bar{T}$ of the three-phase body. As one can see, γ reaches a distinct minimum at $\tilde{T}$ which is a consequence of the "Schreinemakers groove". Below and above $\tilde{T}$, the efficiency of the amphiphile is much lower and differs, as a matter of fact, only little from amphiphile to amphiphile (for a given oil). The determination of such pseudobinary phase diagrams can be handicapped by the existence of lyotropic mesophases (L_α) that extend from the binary water–amphiphile mixture deep into the phase prism. Experiment shows, however, that these mesophases disappear, in general, as one approaches $\tilde{X}$. For reasons of clarity they are, therefore, disregarded in the further discussion, although their existence is a characteristic feature of long-chain amphiphiles.

Except for the extensions of the mesophases, the sections through the three-phase body at $\alpha = 50$ wt % look rather alike for nonionic and ionic amphiphiles. There is, however, an important difference: with nonionics one finds with rising temperature the sequence $\underline{2} \rightarrow 3 \rightarrow \bar{2}$, whereas with ionics one finds $\bar{2} \rightarrow 3 \rightarrow \underline{2}$, which is a consequence of the reverse temperature dependence of the distribution of the amphiphiles between water and oil.

The exact determination of the entire pseudobinary phase diagram can be time consuming. For semiquantitative studies of the dependence of the position and extensions of the three-phase body on the nature of the components and additives one may, therefore, restrict the measurements to determining the coordinates of $\tilde{X}$, that is, $\tilde{T}$ and $\tilde{\gamma}$. Doing so, one, of course, loses the information about T_l and T_u. However, if required, one may choose an amphiphile concentration close to $\tilde{\gamma}/2$ and determine the lower and upper boundaries of the three-phase body at this particular mean composition that gives T_l and T_u in sufficient approximation.

V. Dependence of $\bar{T}$ on the Nature of the Components[7]

For predicting the dependence of the mean temperature $\bar{T}$ of the three-phase body on the nature of the components it suffices to study their effect on the phase diagrams of the binary mixtures. For this purpose it is convenient to apply homologous series of either oils or amphiphiles. As oils we have chosen the series of the *n*-alkanes, characterized by their carbon number k (e.g., B_{10} for *n*-decane). As nonionic amphiphiles we have chosen *n*-alkyl polyglycol ethers, abbreviated as C_iE_j, where i denotes the carbon number of the tail and j the number of ethylene oxide groups of the head. This includes *n*-alcohols (e.g., C_4E_0 for *n*-butyl alcohol). As for ionic amphiphiles, it is more difficult to vary the polarity of the head groups in a systematic manner. For this class of amphiphiles it is, therefore, appropriate to restrict the variation to that of the carbon number of their tails, including the variation of the branching of double-tailed ionic amphiphiles.

The simplest case is that of varying the carbon number k of the oil, because this affects only the binary phase diagram B–C (or D), that is, T_α. As mentioned above, T_α rises with increasing k (for a given amphiphile). This decreases the tendency of nonionic amphiphiles to leave the water-rich phase for the oil-rich phase as one raises T, whereas for ionic amphiphiles it increases their tendency to leave to oil-rich phase for the water-rich phase. With increasing k, accordingly, $\bar{T}$ rises with nonionic amphiphiles, whereas with ionics it drops (Figure 7, top).

Consider now the effect of an added fourth component. The Gibbs–Duhem relation between the variations of the field variables

$$0 = s\delta T - \delta p + \sum c_i \delta \mu_i \qquad \text{(V.1)}$$

states that the effect of temperature (or pressure) on the chemical potentials in a ternary mixture with fixed mean composition can be replaced by adding an appropriate fourth component at constant T and p. At constant pressure, a quaternary mixture has four independent variables. For representing its phase behavior in three-dimensional space, one either has to dispense with temperature by keeping it constant, or to dispense with one of the composition variables by combining two of the components at a fixed ratio into a single "pseudocomponent". If T is kept constant,

(7) For two recently published reviews see: Kahlweit, M.; Strey, R.; Firman, P.; Haase, D.; Jen, J.; Schomäcker, R. *Langmuir* **1988**, *4*, 499; **1989**, *5*, 305.

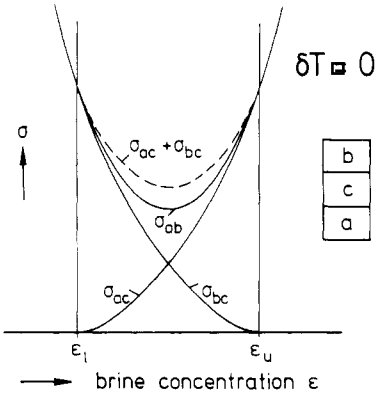

$$0 < \sigma_{ab} \leq \sigma_{ac} + \sigma_{bc}$$

Figure 6. Interfacial tensions between the three phases vs brine concentration ϵ at constant T (schematic).

the phase behavior can be represented exactly in a phase tetrahedron with the A–B–C (or D) triangle as the base, and the fourth component on top. For discussing the temperature dependence, one has to repeat this procedure at various temperatures which is equivalent to moving the tetrahedron up or down the A–B–C (or D) prism like an elevator (see Figure 25 in ref 5). This comes down to determining the temperature dependence of the phase diagrams of four ternary mixtures which can be rather time consuming.

If two of the components are combined into a single component, the phase behavior may be represented in a pseudoternary phase prism with the pseudocomponent placed in one of the corners of the base. It should be emphasized, however, that such a combination will, in general, not behave like a pseudocomponent in the exact sense, that is, like a combination of two components for which the concentration ratio in each of the phases is equal to the mean concentration ratio. The representation of a quaternary mixture in a pseudoternary prism may thus be misleading and should, therefore, be applied with caution. In spite of these reservations we shall, for reasons of convenience, apply the latter representation.

Consider the effect of an added lyotropic salt (E) as, e.g., NaCl. Because salts are practically insoluble in the oil-rich phase, adding salt affects mainly the binary phase diagram A–C (or D). For this reason it is appropriate to consider the mixture of water and salt as a pseudocomponent, defining its composition by the "brine" concentration

$$\epsilon \equiv E/(A + E) \qquad \text{(V.2)}$$

in weight percent. Lyotropic salts "salt out" amphiphiles; that is, they decrease the solubility of amphiphiles in water. With nonionic amphiphiles, this makes the lower critical temperature T_β of their upper loop drop, whereas with ionics it makes the upper critical temperature T_δ of their (lower) miscibility gap rise. With increasing ϵ, accordingly, $\bar{T}$ drops with nonionic amphiphiles, whereas with ionics it rises (Figure 7, center). There is, however, an important difference between nonionic and ionic amphiphiles: with nonionics, the effect of lyotropic salts depends on the nature of the anions, following the "Hofmeister" or "lyotropic series",[8] whereas with ionics, the effect is essentially determined by the ionic strength of the brine, irrespective of the nature of the anions.

As one raises T at constant ϵ, one finds for nonionics the sequence $\underline{2} \rightarrow 3 \rightarrow \bar{2}$, but for ionics again the reverse $\bar{2} \rightarrow 3 \rightarrow \underline{2}$. As one increases ϵ at constant T, one finds in both cases $\underline{2} \rightarrow 3 \rightarrow \bar{2}$. The three-phase triangle appears at a lower brine concentration ϵ_l by separation of the aqueous phase into phases a and c and disappears at an upper brine concentration ϵ_u at which phases b and c merge. Accordingly, the dependence of the interfacial tensions on ϵ at constant T is equivalent to that in a ternary A–B–C mixture on T (Figure 6, to be compared with Figure 2), this being the consequence of the Gibbs–Duhem relation between the variations of the interfacial properties

$$0 = s^\sigma \delta T + \delta\sigma + \sum \Gamma_i \delta\mu_i \qquad \text{(V.3)}$$

which states that the effect of temperature (or pressure) on σ in a ternary mixture with fixed mean composition can be replaced by adding an appropriate fourth component at constant T and p.

Consider now the effect of varying the hydrophobicity of the amphiphile, that is, the (effective) carbon number of its tail (for a given head group). This affects both T_α and T_β. With nonionic amphiphiles, both T_α and T_β drop with increasing hydrophobicity of the amphiphile which makes $\bar{T}$ drop (Figure 7, bottom). With ionics, on the other hand, T_α drops, whereas T_δ rises. Experiment shows that T_α drops more slowly than T_δ rises, so that for ionic amphiphiles $\bar{T}$ rises with increasing hydrophobicity of the amphiphile. Experiment, furthermore, shows that, with both nonionics and ionics, double-tailed amphiphiles or such with branched tails are effectively more hydrophobic than single-tailed amphiphiles with the same carbon number.

Consider, finally, the effect of an added alcohol (C_iE_0). Because alcohols distribute between the water-rich and the oil-rich phase, adding an alcohol affects both the A–C (or D) and the B–C (or D) diagram. Their distribution coefficient depends only weakly on temperature, but sensitively on their carbon number, i, and that of the oil, k. Short-chain alcohols dissolve mainly in the water-rich phase, whereas medium- and long-chain alcohols ($i \geq 4$) show rather wide miscibility gaps with water and thus dissolved mainly in the oil-rich phase. For a qualitative discussion it is, therefore, appropriate to distinguish between the effect of short-chain alcohols and that of long-chain alcohols on $\bar{T}$. Adding a short-chain alcohol that is completely miscible with water increases the mutual solubility between water and amphiphiles. Because this makes T_β rise but T_δ drop, adding a short-chain alcohol is essentially equivalent to decreasing the hydrophobicity of the amphiphile (Figure 7, bottom). Increasing the concentration of a short-chain alcohol thus makes $\bar{T}$ rise with nonionic amphiphiles but drop with ionics. Adding a medium- or long-chain alcohol that dissolves mainly in the oil-rich phase decreases the effective carbon number of the oil, which makes T_α drop. Because the effect on $\bar{T}$ is essentially equivalent to that of decreasing the carbon number of the oil (Figure 7, top), increasing the concentration of a long-chain alcohol thus makes $\bar{T}$ drop with nonionic amphiphiles, but rise with ionic amphiphiles. The higher the i, the more alcohol dissolves in the oil-rich phase, but the smaller the decrease of the effective carbon number of the oil. As a consequence, the effect of adding long-chain alcohols on $\bar{T}$ flattens off with increasing i.

This suggests considering alcohols as "cosolvents", whereas in the literature they are frequently considered as "cosurfactants", the reason being that adding an alcohol at constant temperature may decrease the interfacial tension σ_{ab} between the water-rich and the oil-rich phases. This effect can be readily understood as follows: if the mean temperature of the three-phase body in the alcohol-free mixture does not lie close to the experimental temperature, the two-phase mixture shows a rather high interfacial tension. Adding an alcohol either raises or lowers $\bar{T}$, depending on the nature of the amphiphile. If adding an alcohol makes $\bar{T}$ approach the experimental temperature, σ_{ab} will decrease with increasing alcohol concentration, go through a minimum as $\bar{T}$ becomes identical with the experimental temperature, to increase again as $\bar{T}$ passes the experimental temperature. This process is thus equivalent to that shown on Figure 6, the alcohol concentration playing the role of ϵ. Because the minimum of the interfacial tension coincides with the maximum of the mutual solubility between water and oil, the latter will pass a maximum at the same alcohol concentration.

The general patterns of the dependence of $\bar{T}$ on the (effective) carbon number of the oil (for a given amphiphile), on the concentration of (lyotropic) salts (for a given amphiphile and oil),

(8) See, e.g.: Firman, P.; Haase, D.; Jen, J.; Kahlweit, M.; Strey, R. *Langmuir* **1985**, *1*, 718.

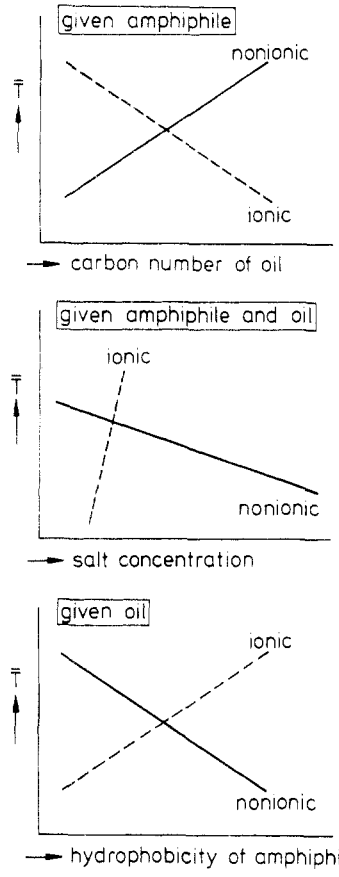

Figure 7. Dependence of $\bar{T}$ on carbon number k of the oil (top), brine concentration ϵ (center), and hydrophobicity of the amphiphile (bottom; all schematic).

and on the (effective) carbon number of the tail group of the amphiphile (for a given oil and head group) are schematically summarized on Figure 7. As one can see, the phase behavior of nonionic and ionic amphiphiles is in every respect reverse. This also holds for the dependence of $\bar{T}$ on pressure: with nonionics, the three-phase bodies rise and widen with increasing pressure, whereas with ionics, they drop and shrink.[9]

For the discussion of the phase behavior of quinary mixtures (A + E)–B–(C + D) with mixtures of nonionic and ionic amphiphiles as they are frequently applied in practice the reader is referred to ref 10.

VI. An Experimental Example

The strong relation between the critical temperatures of the miscibility gaps of the binary mixtures and the mean temperature of the three-phase body is demonstrated in Figure 8 for the ternary mixture A–B_k–C_8E_j. In the center, on the left, one can see the dependence of T_β on j in the binary A–C_8E_j mixtures. As already mentioned in section III, T_β rises with increasing j, that is, increasing hydrophilicity of the amphiphile (at fixed i). On the right one can see the dependence of T_α on k for some binary B_k–C_iE_5 mixtures. As already mentioned in section III, T_α rises with increasing k (for a given C_iE_5), but drops with increasing i (at fixed k). On the lower left one can see the dependence of $\bar{T}$ on j for A–B_k–C_8E_j mixtures, with k as parameter. The curves show the same slope as the one for the oil-free mixture, slightly shifted with respect to temperature, which indicates a rather weak effect of the oil on the interaction energies between water and amphiphile. On the lower right one can see the dependence of $\bar{T}$ on k, with j as parameter. The curves show weaker slopes than those for the water-free mixtures and are shifted toward higher temperatures, which indicates a rather strong effect of water on the interaction energies between oil and amphiphile.

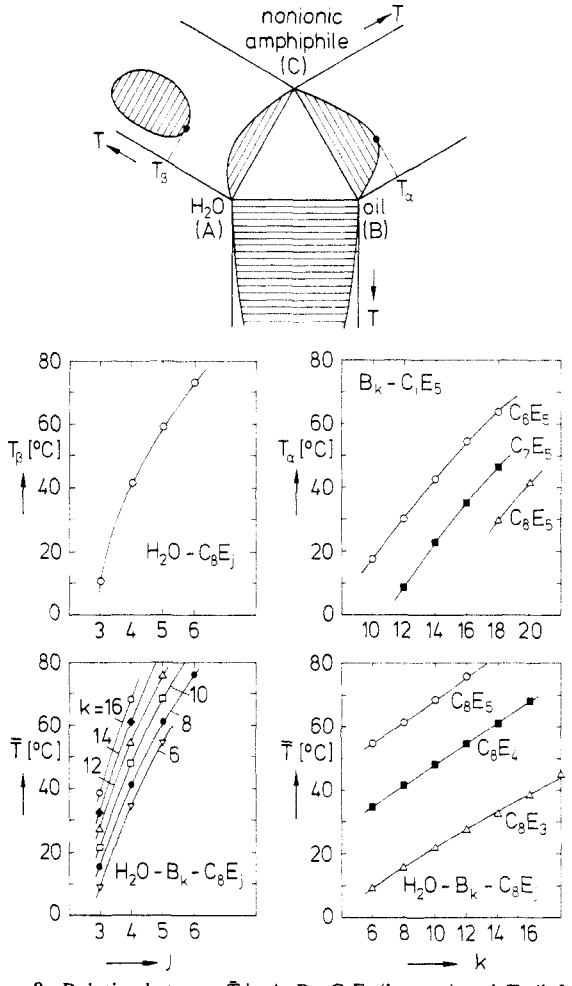

Figure 8. Relation between $\bar{T}$ in A–B_k–C_8E_j (bottom) and T_β (left) or T_α (right).

This obvious relation between the critical temperatures of the binary phase diagrams and the mean temperature of the three-phase body demonstrates convincingly that any realistic expression for the Gibbs free energy of such mixtures must include the temperature dependence of the interaction energies between the components as it manifests itself in the corresponding binary mixtures. This is, however, only necessary but not sufficient for describing the properties of microemulsions because any ternary mixture which exhibits a similar temperature dependence of the interaction energies as, e.g., mixtures with short-chain amphiphiles, will, evidently, show a similar relation between the features of the binary mixtures and $\bar{T}$.[11]

VII. Microemulsions

"Microemulsions" were viewed by Schulman[12] as "optically isotropic, fluid, transparent oil and water dispersions, consisting of uniform droplets of either oil or water in the appropriate continuous phase". Today one knows that the homogeneous mixtures of water, oils, and amphiphiles may show various microstructures, ranging from weakly structured solutions to spongelike structures with water and oil domains with diameters of the order of 10 nm, apparently separted by saturated monolayers of the amphiphile. This makes drawing a border line between weakly structured mixtures and microemulsions difficult. Widom[13] suggested "seeing that difference reflected in the wetting vs nonwetting of the oil–water interface by the middle phase", that

(9) Reference 7. See also: Sassen, C. L.; Filemon, L. M.; de Loos, Th. W.; de Swaan Arons, J. *J. Phys. Chem.* **1989**, *93*, 6511.
(10) Kahlweit, M.; Strey, R. *J. Phys. Chem.* **1988**, *92*, 1557.
(11) See, e.g.: Lang, J. C.; Widom, B. *Physica A* **1975**, *81*, 190. Knickerbocker, B. M.; Pesheck, C. V.; Scriven, L. E.; Davis, H. T. *J. Phys. Chem.* **1979**, *83*, 1979. Kahlweit, M. *J. Colloid Interface Sci.* **1982**, *90*, 197.
(12) Schulman, J. H.; Stoeckenius, W.; Prince, L. M. *J. Phys. Chem.* **1959**, *53*, 1677.
(13) Widom, B. *Langmuir* **1987**, *3*, 12.

is, in the equality vs inequality in eq II.3. This, again, does not appear to be sufficient. As will be shown in the following section, the incomplete wetting of the interface between the polar and the nonpolar bulk phase is not a particular property of the ternary mixture but exhibits itself already in the oil-free mixture. Experiment, furthermore, shows the domain size at $\tilde{X}$ to increase with increasing efficiency of the amphiphile, that is, decreasing amount of amphiphile required for homogenizing equal masses of water and oil. The efficiency, however, depends not only on the nature of the amphiphile, but also on that of the oil and, in particular, on temperature, reaching its maximum in the three-phase temperature interval. Accordingly, one expects the largest domains to be found at temperatures near $\bar{T}$ and at mean compositions close to the binodal surface. The larger the difference between the experimental temperature and $\bar{T}$, the lower the efficiency of the amphiphile and the smaller thus the domain size.

Although choosing $\bar{T}$ as the experimental temperature facilitates preparing a microemulsion of a particular mixture, this is again not sufficient. Consider, for example, ternary A–B_{10}–C_iE_j mixtures with C_6E_3, C_8E_4, $C_{10}E_5$, and $C_{12}E_6$ as nonionic amphiphiles.[14] All mixtures exhibit the phase behavior as described in the previous sections, with three-phase bodies at $\bar{T} \approx 50$ °C; and in all mixtures the middle phase does not wet the a/b interface. But, with C_6E_3 one requires $\tilde{\gamma} \approx 50$ wt % of amphiphile for homogenizing equal masses of water and oil, whereas with $C_{12}E_6$ about 10 wt % suffices. Similar considerations hold if the carbon number k of the oil is varied with a given amphiphile. This is demonstrated in Figure 2 in ref 6 that shows $\tilde{\gamma}$ vs k for A–B_k–C_8E_4 mixtures. With hexane, about 20 wt % of amphiphile suffices, whereas with hexadecane about 50 wt % is required.

This raises the question as to what determines the stability of colloidal dispersions. A first attempt to find an answer was made by Volmer[15] in 1931, and a second in 1956 on the basis of kinetic considerations. He found the droplet size in a stable dispersion of the solute in a binary liquid mixture to be determined by the interfacial tension σ between the two bulk phases and predicted a rather narrow size distribution of the droplets with a mean radius at

$$r^2\sigma/(k_BT) = 7/4\pi \qquad \text{(VII.1)}$$

Equivalent relations were thereafter derived by Rehbinder[16] and, independently, by Reiss[17] on the basis of thermodynamic considerations, namely by balancing the tendency of the interfacial tension to decrease the interfacial area of the dispersion with the counteracting tendency of entropy to disperse the solute. The problem with this approach is, evidently, to calculate the entropy of mixing of a dispersion. By applying the hard-sphere model, Reiss found

$$r^2\sigma/(k_BT) = (4\pi)^{-1}[(5/2) - (3/2)/(1-\Phi)^2 + \ln\{(16r^3/v_i)^{3/2}(1-\Phi)/\Phi\}] \qquad \text{(VII.2)}$$

where Φ is the volume fraction and v_i the volume per molecule of the dispersed solute. The right-hand side of eq VII.2 is of the order of unity, depending only weakly on r and Φ. On top of Figure 9, $(r^2\sigma/k_BT)$ is plotted vs r, with Φ as parameter, and $v_i = 3 \times 10^{-23}$ cm^3 (corresponding to H_2O as dispersed solute). For semiquantitative calculations one may, therefore, set

$$r^2\sigma/(k_BT) \approx 1 \qquad \text{(VII.3)}$$

The error introduced by this approximation depends only weakly on σ as can be seen at the bottom of Figure 9 which shows r vs σ as evaluated from eq VII.2, setting $k_BT = 4.14 \times 10^{-14}$ erg, $\Phi = 0.5$, and $v_A = 3 \times 10^{-23}$ cm^3 (corresponding to H_2O as solute), or $v_B = 3 \times 10^{-22}$ cm^3 (corresponding to a medium-chain alkane). The broken line represents r as evaluated from eq VII.3. For σ

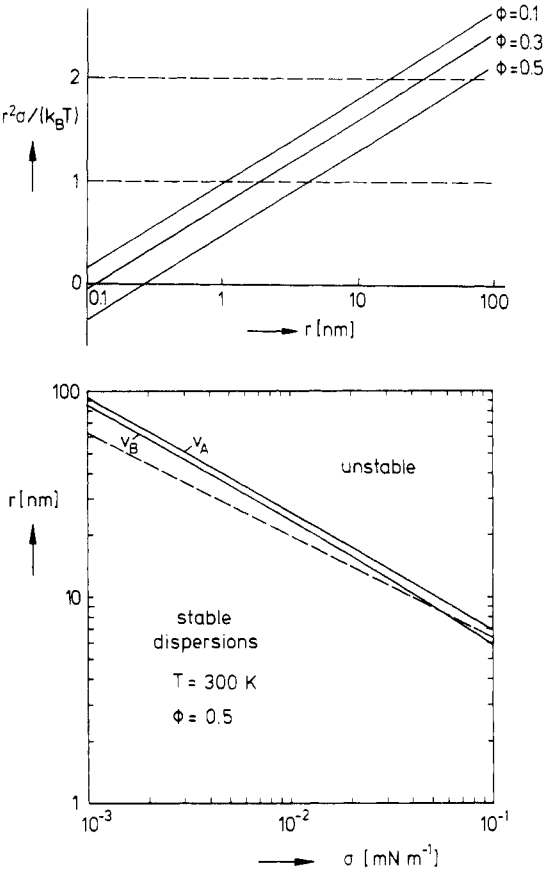

Figure 9. (Top) $r^2\sigma/(k_BT)$ vs r, with Φ as parameter, after eq VII.2. Bottom: Droplet radius r vs interfacial tension σ after eq VII.2 (full lines) and after eq VII.3 (broken line).

$= 1$ mN m^{-1}, i.e., $r \approx 1$ nm, one can hardly speak of a colloidal dispersion. However, as σ decreases below 10^{-1} mN m^{-1}, the radii of the droplets become 5 nm and larger so that the droplets can be considered as macroscopic domains of the solute.

This suggests defining microemulsions as stable colloidal dispersions of domains of either oil or water sufficiently large for the dispersed solute to exhibit the properties as, e.g., the dielectric number of a bulk phase. It, furthermore, suggests relating the efficiency of an amphiphile to the interfacial tension σ_{ab} of a plane interface between the water-rich and the oil-rich phase in the presence of a saturated monolayer. The interfacial tension between water and oil is about 50 mN m^{-1}. But, as Hoar and Schulman[18] realized already in 1943, the spontaneous emulsification of the two solvents is made possible by the lowering of the interfacial tension σ_{ab} due to the adsorption of an amphiphile at their interface. The tendency to adsorb, and thus the lowering of σ_{ab}, increases with increasing amphiphilicity. Figure 10 shows on its lower left the σ_{ab}/log γ curve for the A–benzene–ethanol (C_2E_0) mixture, measured at 25 °C along the path shown on the upper left.[19] Although ethanol can be considered as a weak amphiphile, the curve shows a sigmoidal shape with σ_{ab} dropping below 1 mN m^{-1} only close to the plait point ($\gamma = 36.8$ wt %). The lower right shows the corresponding curve for the A–B_8–C_6E_3 mixture, measured at 34 °C along the path shown on the upper right ($\alpha = 50$ wt %). σ_{ab} drops steeply to 0.32 mN m^{-1} at $\gamma = 2.5$ wt % well below the plait point, to remain constant up to $\gamma = 20$ wt %. Such a break in the slope of a σ_{ab}/log γ curve was first found by Powney and Addison in 1937[20] in a ternary mixture with an ionic amphiphile. As will be shown in the following section, this break represents a point on the "cmc surface" at this particular temperature and α. The mixture with the short-chain C_2E_0 (Figure 10) does not show such a break, whereas that with the

(14) See Figure 3 in: Kahlweit, M.; Strey, R.; Firman, P. *J. Phys. Chem.* **1986**, *90*, 671.
(15) Volmer, M. *Z. Phys. Chem.* **1931**, *155*, 281; **1957**, *206*, 181.
(16) Shchukin, E. D.; Rehbinder, P. A. *Colloid J. USSR (Engl.)* **1958**, *20*, 601.
(17) Reiss, H. *J. Colloid Interface Sci.* **1975**, *53*, 61.
(18) Hoar, T. P.; Schulman, J. H. *Nature* **1943**, *152*, 102.
(19) Wielebinski, D.; Findenegg, G. H. *J. Phys. Chem.* **1984**, *88*, 4397.
(20) Powney, J.; Addison, C. C. *Trans. Faraday Soc.* **1937**, *33*, 1243.

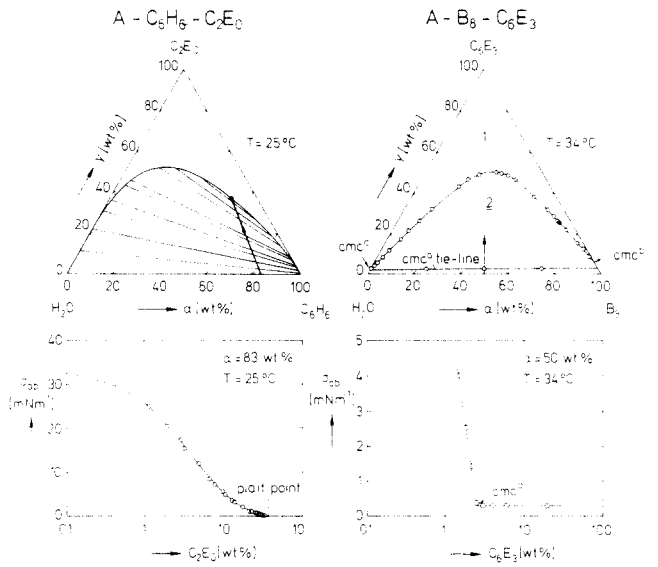

Figure 10. (Left) Interfacial tension σ_{ab} vs log γ in A–C_6H_6–ethanol,[19] measured along the path shown on top. (Right) Interfacial tension σ_{ab} vs log γ in A–B_8–C_6E_3, measured at α = 50 wt %. The cmc[a] tie line was determined by measuring the break of the σ_{ab}/log γ curve at α = 25 and 75 wt %.

medium-chain C_6E_3 does. As one increases the amphiphilicity further, the break moves to lower amphiphile concentrations, with σ_{ab} at that break decreasing to values $<10^{-2}$ mN m^{-1} with long-chain amphiphiles. This suggests the existence of a distinct cmc to be a necessary condition for preparing a microemulsion, because only then may the interfacial tension σ_{ab} drop to sufficiently low values at low amphiphile concentrations. The interfacial tension may then be lowered further by choosing a temperature near the mean temperature $\bar{T}$ of the three-phase body, at which σ_{ab} reaches its minimum. Experiment shows that the tendency to form micelles increases gradually with increasing amphiphilicity. With nonionic *n*-alkyl polyglycol ethers, the medium-chain C_6E_j's appear to be the first that show a distinct cmc, although the value of σ_{ab} is still too high to expect microemulsions in the above narrower sense. However, the higher the amphiphilicity the more likely may one find microemulsions not only near $\bar{T}$, but also at temperatures above and below the three-phase body, at which σ_{ab} is sufficiently low.

A semiquantitative relation between the efficiency of an amphiphile and σ_{ab} may then be derived as follows: If the thickness of the interfacial layer is neglected, the volume fraction Φ of the dispersed phase is

$$\Phi = N_v(4\pi/3)r^3 \qquad \text{(VII.4)}$$

where N_v is the number density of droplets. The interfacial area per unit volume A_v is

$$A_v = N_v 4\pi r^2 \qquad \text{(VII.5)}$$

so that

$$\Phi/A_v = r/3 \qquad \text{(VII.6)}$$

The internal interface A_v can be obtained from the mass balance of the amphiphile which reads per unit volume

$$c = c^* + \Gamma A_v \qquad \text{(VII.7)}$$

where c^* denotes the amphiphile concentration at the cmc surface at the chosen T and α, and Γ is the interfacial concentration of the amphiphile in the saturated water/oil interface. Combination of eqs VII.3, VII.6, and VII.7 yields

$$c - c^* = 3\Phi\Gamma\{\sigma_{ab}/(k_BT)\}^{1/2} \qquad \text{(VII.8)}$$

where c now denotes the minimum concentration of amphiphile required for homogenizing the mixture. Equation VII.8 contains only measurable quantities. Γ, in particular, can be obtained from the slope of the σ_{ab}/log γ curve at the cmc by applying Gibbs' adsorption isotherm (eq V.3 with $\delta T = \delta p = 0$). In aqueous solutions of single-tailed medium- and long-chain nonionic amphiphiles, one finds at ambient temperatures $(\partial\sigma/\partial \log \gamma)_{cmc} \approx -20$ mN m^{-1}. Assuming $\Gamma_A = 0$, this gives $\Gamma_C \approx 3.5 \times 10^{-10}$ mol cm^{-2}. In ternary A–B_k–C_iE_j mixtures with medium-chain amphiphiles one finds $(\partial\sigma_{ab}/\partial \log \gamma)_{cmc} \approx -15$ mN m^{-1}. If one again assumes for a saturated monolayer $\Gamma_A = \Gamma_B = 0$, this gives $\Gamma_C \approx 2.6 \times 10^{-10}$ mol cm^{-2}, which would indicate that the effective area occupied by each amphiphile molecule at the water/oil interface is somewhat larger than at the water/air interface.

For estimating the minimum amount $\tilde{\gamma}$ of amphiphile required for homogenizing equal masses of water and oil (α = 50 wt %) near the mean temperature $\bar{T}$ of the three-phase body, one may set in eq VII.8 $\Phi = 0.5$, $\Gamma = 3 \times 10^{-10}$ mol cm^{-2}, $\sigma_{ab} = 10^{-2}$ mN m^{-1}, and $k_BT = 4 \times 10^{-14}$ erg, to find $(c - c^*) = 2.25 \times 10^{-4}$ mol cm^{-3}. The relation between c and γ is

$$c = 10^{-2}\gamma\bar{\rho}/M_c \qquad \text{(VII.9)}$$

where M_c denotes the molar mass of the amphiphile and $\bar{\rho}$ the mean density of the mixture. Setting $M_c = 4 \times 10^2$ g mol^{-1} and $\bar{\rho} = 1$ g cm^{-3}, one finds, neglecting c^*, $\tilde{\gamma} = 9$ wt %, which is of the experimentally observed magnitude.

VIII. The Cmc Surfaces

In aqueous solutions, "micelle formation is a property parallel to interfacial tension reduction", and "in fact competitive".[21] Experiment shows that, at low amphiphile concentrations, the binary A–C (or D) mixture lowers its free energy by accumulating the amphiphilic molecules at the water/air interface which indicates that, at low concentrations, the change of the Gibbs free energy of the solution by adsorption, $-\Delta G_{ad}$, is higher than that of micellization, $-\Delta G_{mic}$. This leads to a strong decrease of the interfacial tension from $\approx$72 mN m^{-1} to that of an oil/air interface ($\approx$30 mN m^{-1}). With increasing amphiphile concentration, however, it becomes energetically more favorable to expel the amphiphile by forming micelles rather than by squeezing additional molecules into the interfacial layer. Accordingly, one may define the critical micelle concentration (cmc) by

$$0 = (\Delta G_{ad} - \Delta G_{mic})_{cmc} \qquad \text{(VIII.1)}$$

Above the cmc, $-\Delta G_{ad}$ is lower than $-\Delta G_{mic}$, so that the system lowers its free energy by forming micelles. As a consequence, the concentration of the monomers remains practically constant above the cmc. Because micelles are symmetrically hydrophilic, they do not adsorb at the interface, so that the interfacial concentration remains practically constant above the cmc, as does the interfacial tension. If traces of oil are present, this catalyzes micelle formation which makes the cmc decrease.

If the hydrophilic interaction between the head groups and water becomes too weak, micelles separate as a second bulk phase. Because, with nonionic amphiphiles, the hydrophilic interaction decreases with rising temperature, nonionic micelles separate at elevated temperatures which gives rise to the upper loop in A–C mixtures. With ionic amphiphiles, however, the hydrophilic interaction decreases with dropping temperature which gives rise to the lower miscibility gaps in A–D mixtures.

For reasons of clarity, the following considerations are restricted to mixtures with nonionic amphiphiles. Hitherto, the cmc's in aqueous solutions of nonionic amphiphiles were determined only at temperatures below T_β. The results show that the cmc decreases slightly with rising temperature, shaping an almost vertical curve running toward the water-rich side of the upper loop. This raises the question as to whether the curve passes the loop on its water-rich side, or whether it intersects with the loop. For answering this question experimentally, the amphiphiles have to be very pure because even traces of impurities stemming from their synthesis may catalyze micellization. After careful purification one finds the cmc curve to pass the loop on its water-rich side up to temperatures near the boiling temperature (see Figure 13). This was apparently first shown by Corti, Degiorgio, and Zulauf[22] on

(21) Hartley, G. S. *Trans. Faraday Soc.* **1941**, *37*, 130.

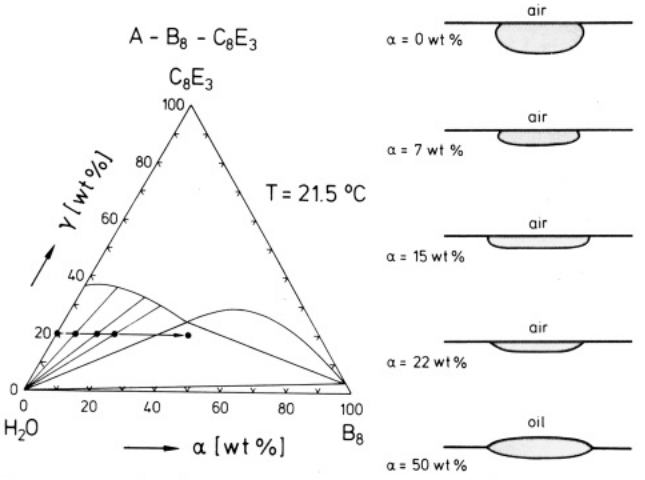

Figure 11. Profile of a droplet of the amphiphile-rich phase, proceeding from the oil-free mixture (top) into the three-phase triangle (bottom).

the A–C_8E_4 mixture. Whether or not the curve passes the entire loop can, at present, not be answered because the upper critical points in the loops lie, in general, well above the boiling temperature. From this it follows that the amphiphile-rich phase of the loop is in equilibrium with a micellar solution on the water-rich side. In this context it should be emphasized that the microstructure of the isotropic (!) amphiphile-rich phase is still not clear. All that can be said from wetting experiments is that a drop of the upper amphiphile-rich phase does not spread across the liquid/air interface but contracts to a lens.[23] The incomplete wetting of the water/oil interface in the ternary mixture is thus not a particular property of the amphiphile-rich phase (c) but exhibits itself already in the oil-free mixture. This is demonstrated in Figure 11 that shows on its right the change of shape of the lens of the amphiphile-rich phase of the A–B_{10}–C_8E_3 mixture as one proceeds at 21.5 °C ($\approx \tilde{T}$) isothermally from the oil-free mixture through the two-phase region into the three-phase triangle along the path shown on the left.

In the oil-free mixture ($\alpha = 0$), the cmc curve ascends almost vertically along the A–C side of the phase prism. As one adds oil, the curve proceeds through the narrow region in the homogeneous water-rich phase a until it terminates at the cmc^a curve ascending on the water-rich side of the body of heterogeneous phases, thus shaping an almost vertical cmc surface within phase a. At amphiphile concentrations below that surface, the amphiphile is molecularly disperse. At concentrations above the cmc^a surface, the concentration of monomers remains practically constant, whereas the number density of micelles increases, at first, lineary with increasing amphiphile concentration. Because the micelles solubilize oil, this leads to an increase of the apparent solubility of oil in phase a which exhibits itself in a discontinuity of the (isothermal) slope of the binodal at cmc^a. This discontinuity is difficult to detect due to the very low cmc's in phase a. Precise determinations of the binodals in mixtures with medium-chain nonionic amphiphiles, that is, with relatively high cmc's, however, reveal that the binodals show a straight portion above cmc^a the extrapolation of which does not terminate at the H_2O corner but at a value close to that of the cmc in the oil-free mixture. This is demonstrated on the lower left of Figure 12 which shows the binodal of the A–B_8–C_6E_3 mixture in the water-rich corner of the phase prism at 34 °C, that is, just below T_l of that mixture. Each point on the cmc^a curve is connected by a tie line with a point on the oil-rich side of the binodal surface. These cmc^a tie lines shape an almost vertical, somewhat tilted surface within the body of heterogeneous phases that terminates at the oil-rich side of the binodal surface.

Consider now the situation in the oil-rich homogeneous phase. Solutions of amphiphiles in nonpolar solvents differ from aqueous

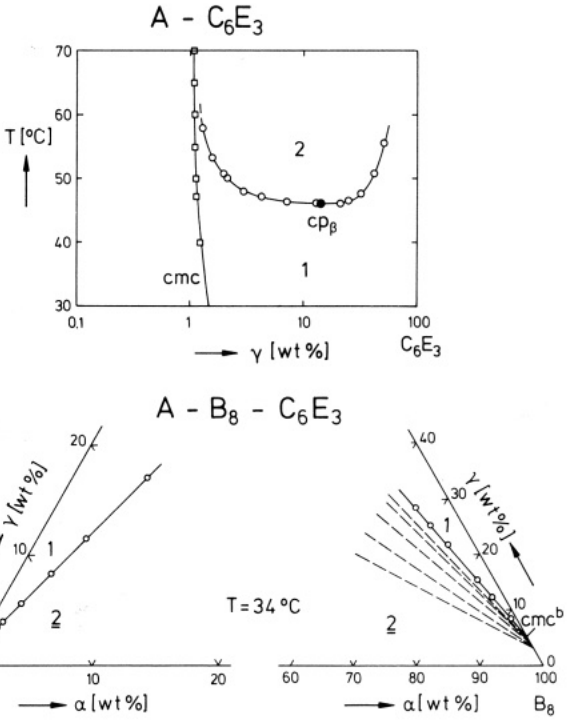

Figure 12. (Top) Phase diagram of A–C_6E_3 with cmc and upper loop. (Bottom) Straight portions of the binodal in the water-rich (left) and oil-rich (right) corner in A–B_8–C_6E_3, defining cmc^a and cmc^b. The broken lines on the lower right represent some experimentally determined tie lines.

solutions insofar as amphiphiles do not adsorb at oil/air interfaces because air must be considered as a nonpolar phase in this respect. The cmc in such solutions can, therefore, not be determined by interfacial tension measurements. Whether or not (inverse) micelles form in "dry" nonpolar solvents is still controversial. Experiments in water-free B_k–C_iE_j mixtures indicate that, at low amphiphile concentrations, the degree of association is low and only small aggregates exist.[24] If, however, traces of water are present, the mixture lowers its free energy by forming micelles in the oil-rich phase b. The structure as well as aggregation number of these micelles differs from that in aqueous solutions. Because, furthermore, the driving force for forming micelles in phase b will depend on the water concentration, that is, on the degree of hydration of the head groups, $-\Delta G_{mic}$ in oil (with traces of water) will differ from that in water.

The situation is best defined on the oil-rich side of the binodal surface, that is, in phase b saturated with water. Again cmc^b will shape an almost vertical curve ascending along the binodal surface. Because inverse micelles solubilize water, this leads to an increase of the apparent solubility of water in phase b which exhibits itself in a discontinuity of the slope of the binodal. Such discontinuities were first found by Kunieda and Shinoda[25] in 1982 in A–B_{14}–$C_{12}E_5$ mixtures, although their significance was apparently not recognized at that time. Again the binodals show a straight portion above cmc^b the extrapolation of which does not terminate at the oil corner but at an amphiphile concentration distinctly higher than zero on the B–C side of the phase prism. This is demonstrated on the lower right of Figure 12 which shows the binodal of the A–B_8–C_6E_3 mixture in the oil-rich corner of the phase prism at 34 °C, with $cmc^b \approx 5.6$ wt %. Each point on the cmc^b curve is connected by a tie line with a point on the water-rich side of the binodal surface. These cmc^b tie lines shape an almost vertical, somewhat tilted surface within the body of heterogeneous phases that terminates at the water-rich side of the binodal surface. The broken lines on the lower right of Figure 12 represent tie lines

(22) Corti, M.; Degiorgio, V.; Zulauf, M. *Phys. Rev. Lett.* **1982**, *48*, 1617.
(23) Kahlweit, M.; Busse, G. *J. Chem. Phys.* **1989**, *91*, 1339.
(24) Jones, P.; Wyn-Jones, E.; Tiddy, G. J. T. *J. Chem. Soc., Faraday Trans. 1* **1987**, *83*, 2735.
(25) Kunieda, H.; Shinoda, K. *J. Disp. Sci. Technol.* **1982**, *3*, 233.

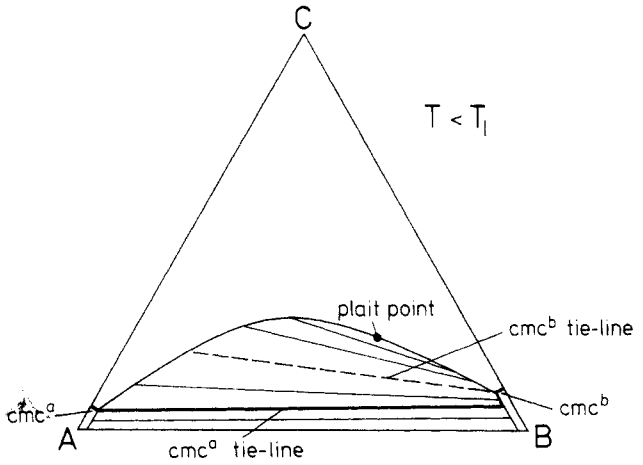

Figure 13. Isothermal section through phase prism at $T < T_l$ with cmc^a tie line, cmc^b tie line, and section through cmc surface (thick line, all schematic).

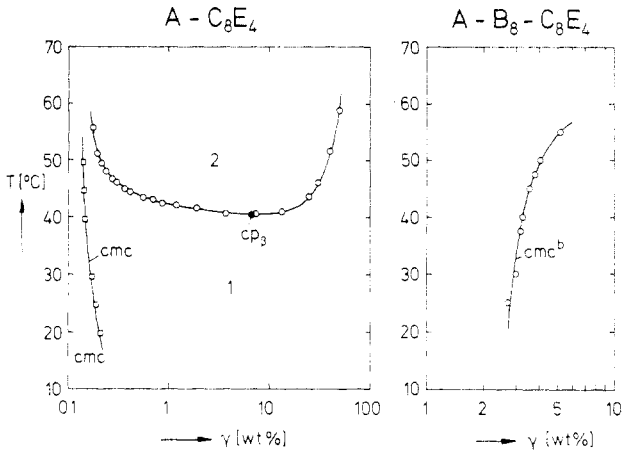

Figure 14. Temperature dependence of cmc^a and cmc^b. (Left) Phase diagram of A–C_8E_4 with cmc ≈ cmc^a. (Right) cmc^b vs T in A–B_8–C_8E_4.

that were determined by measuring the refractive indexes of the two coexisting phases and comparing them with the refractive indexes measured in the homogeneous phase along the binodal. All measured tie lines terminate at concentrations below cmc^b, indicating that the actual cmc^b tie line ascends very steeply.

In the narrow region of the homogeneous oil-rich phase (b), on the other hand, the cmc^b curve proceeds toward the water-free side of the phase prism. Because the tendency to form micelles decreases with decreasing water concentration, the cmc surface may become increasingly more diffuse as the water concentration approaches zero. At amphiphile concentration below that surface, the amphiphile is molecularly disperse. At concentrations above the cmc^b surface, the concentration of monomers remains practically constant, whereas the number density of inverse micelles increases, at first, linearly with increasing amphiphile concentration.

To summarize, ternary A–B–C mixtures show two cmc curves, the cmc^a curve ascending on the water-rich side and the cmc^b curve ascending on the oil-rich side of the binodal surface. Each curve represents the intersection of a cmc surface with the binodal surface. The cmc^a surface starts at the cmc curve of the binary A–C mixture, proceeds toward the cmc^a curve, and passes through the body of heterogeneous phases along the cmc^a tie lines, to terminate at a curve ascending on the oil-rich side of the binodal surface. The cmc^b surface may be somewhat diffuse in the water-free mixture, but becomes well-defined at the cmc^b curve on the oil-rich side of the binodal surface from where it passes through the body of heterogeneous phases along the cmc^b tie lines, to terminate at a curve ascending on the water-rich side of the binodal surface. Because the free energy of micelle formation will be different on the water-rich and the oil-rich side of the binodal surface, the two cmc surfaces will, in general, not coincide. Both the cmc^a and the cmc^b curve can, in principle, be determined by precise measurements of isothermal sections through the binodal surface in the corresponding corner of the phase prism. In practice, however, cmc^a may be set equal to the cmc in the oil-free mixture where it can be determined by interfacial tension measurements, whereas cmc^b can be determined readily by measuring the discontinuity of the slope of the binodal on the oil-rich side which is facilitated by the fact that, for nonionic amphiphiles, cmc^b is considerably higher than cmc^a. Figure 13 shows a schematic isothermal section through the phase prism of an A–B–C mixture at a temperature below T_l, that is, with the tie lines declining toward the B corner (2). The thick line represents the section through the cmc surface, being identical with the cmc^a tie line within the central miscibility gap. At mean compositions below the thick line, one finds molecularly disperse solutions only. At compositions between the thick line and the cmc^b tie line, one finds micelles in the water-rich phase only, whereas at compositions above the cmc^b tie line, one finds micelles in both the water-rich and the oil-rich phases.

IX. Temperature Dependence of Cmc^a and Cmc^b

Because the cmc^a curve is difficult to measure, one has to assume it to be practically equal to the cmc in the oil-free binary A–C mixture. Figure 14 shows on its left the phase diagram of the binary A–C_8E_4 mixture with the cmc curve. The cmc in the oil-free mixture decreases with rising temperature. The derivative $\partial \log \text{cmc}/\partial\,(1/T)$, being a measure for the enthalpy of micellization, is thus positive, decreasing, however, with increasing $1/T$.

The temperature dependence of cmc^b, on the other hand, can be readily determined by precisely measuring the straight portions of the binodals on the oil-rich side, and setting the intersection between these straight portions and the B–C side of the Gibbs triangle equal to cmc^b. The result for the A–B_8–C_8E_4 mixture is shown on the right of Figure 14. Cmc^b increases with rising temperature. $\partial \log \text{cmc}^b/\partial(1/T)$ is thus negative, decreasing too with increasing $1/T$. This appears to hold for all nonionic amphiphiles hitherto studied.

The cmc^b tie lines decline toward the oil corner for $T < T_l$ (2) but toward the H_2O corner for $T > T_u$ ($\bar{2}$). Because cmc^a is, in general, lower than cmc^b, one, accordingly, expects the cmc^a surface for $T < T_l$ to lie at lower amphiphile concentrations than the cmc^b surface (as shown on Figure 13). For $T > T_u$, however, the reverse is true as will be shown in the following section.

X. Evolution of the Three-Phase Triangle

On the basis of the previous sections one may now discuss the position of the three-phase body with respect to the two cmc surfaces. This can be done by erecting two vertical sections through the oil-rich corner of the phase prism as shown on top of Figure 15 for the A–B_8–C_8E_4 mixture. This yields two vertical sections through the three-phase body in that corner, from which one may construct the oil-rich corners of the three-phase triangles as they change with temperature. The result is shown on the left of Figure 15. For reasons that will become clear later, it is convenient to discuss the evolution of the three-phase triangles on the oil-rich side starting at T_u, and lowering temperature. At 48 °C (upper left), that is, just below T_u, the oil-rich corner (b) of the three-phase triangle lies at an amphiphile concentration above that of cmc^b. Consequently, the cmc^b tie line must pass through the two-phase region adjacent to the b–a side of the triangle. One thus deduces that the upper critical tie line of the three-phase body lies between the cmc^b and the cmc^a tie line as shown schematically on the upper right, with the cmc^a tie line passing through the two-phase region above the critical tie line. As a consequence, the critical end point cep$_\alpha$ on the oil-rich side at which the (inverse) micellar solution separates into phases b and c lies between cmc^b and the oil-rich point of the cmc^a tie line, being in equilibrium with a molecularly disperse solution on the water-rich side. With further dropping of temperature, both phase b and cmc^b move toward the oil corner. Phase b, however, moves faster than cmc^b as shown schematically on the right of Figure 16, and thus overtakes cmc^b at some temperature near $\bar{T}$ (Figure

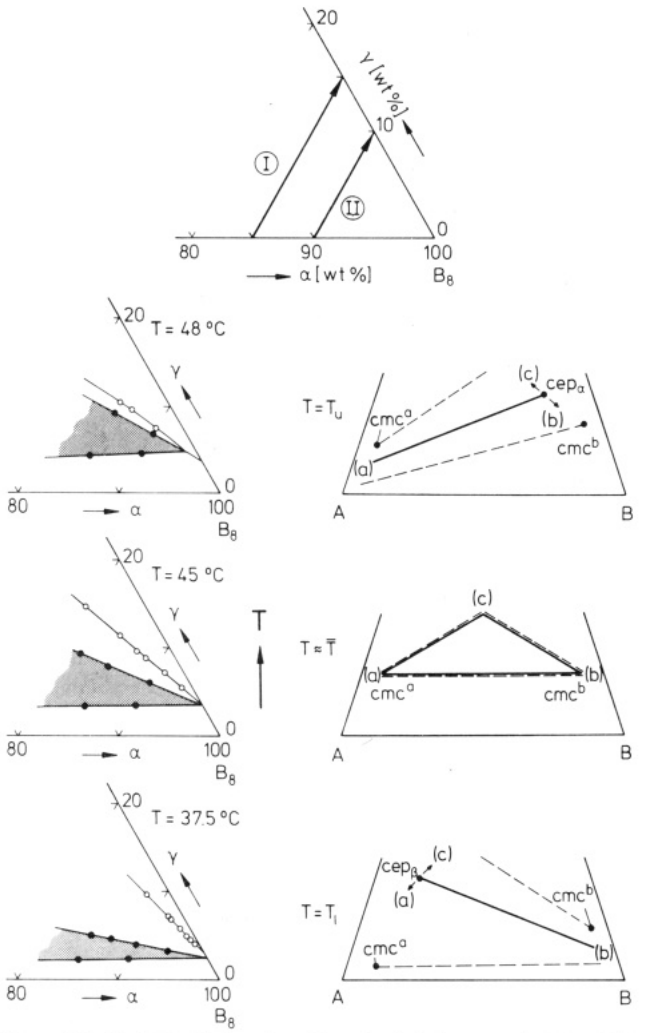

Figure 15. (Top) Vertical sections through oil-rich corner of $A-B_8-C_8E_4$ prism, yielding the oil-rich corners of the three-phase triangles shown on the lower left. (Lower right) Position of upper critical tie line (top), symmetrical triangle (center), and lower critical tie line (bottom) with respect to cmc^a and cmc^b tie lines, respectively (schematic).

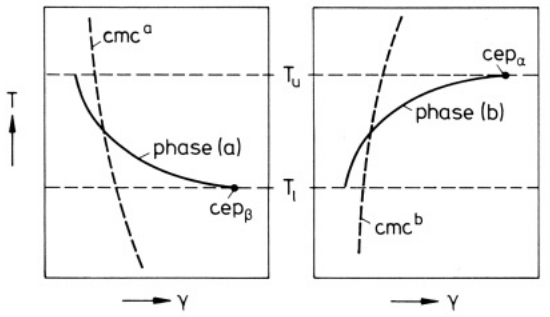

Figure 16. Trajectories of cmc^a and water-rich phase (a) (left) and of cmc^b and oil-rich phase (b) (right), projected onto the A–C or B–C plane, respectively (schematic).

15, center left). At this temperature (≈45 °C), cmc^b has two tie lines. The first one coincides with the b–a side of the triangle, whereas the second one coincides with the b–c side of the three-phase triangle (Figure 15, center right). Assuming the evolution of the water-rich side to be symmetrical but reverse with respect to temperature, phase a coincides with cmc^a at the same temperature, so that cmc^a, too, has two tie lines, namely the a–b and the a–c side of the triangle. At this temperature, phase c is in equilibrium with both cmc^a and cmc^b. At 37.5 °C (Figure 15, lower left), that is, just above T_l, phase b lies below cmc^b. Consequently, the cmc^b tie line must pass through the two-phase region adjacent to the b–c side of the three-phase triangle. One thus deduces that the lower critical tie line of the three-phase body lies between the cmc^a and the cmc^b tie line at T_l (bottom, right), the first one passing through the two-phase region below the critical tie line and the latter through the one above the critical tie line. The position of the two cmc tie lies at T_l with respect to the critical tie line is thus reverse of that at T_u. This also holds for the critical end point cep_β on the water-rich side of the lower critical tie line at which the micellar solution separates into phases a and c. It lies between cmc^a and the water-rich point of the cmc^b tie line, being in equilibrium with a molecular disperse solution on the oil-rich side.

As one starts at T_l, raising temperature, the evolution of the three-phase triangles on the water-rich side may be assumed to be symmetrical but reverse with respect to temperature. With rising temperature, both phase a and cmc^a move toward the water corner. Phase a, however, moves faster than cmc^a (Figure 16, left) and overtakes cmc^a near $\bar{T}$. At this temperature, cmc^a has two tie lines. The first one coincides with the a–b side of the triangle and, at the same time, with one of the two cmc^b tie lines, whereas the second one coincides with the a–c side of the triangle. With further rise in temperature, cmc^a lies above phase a, so that the latter is molecularly disperse.

The schematical diagrams on the right of Figure 15 and in Figure 16 were drawn symmetrically with respect to concentrations. In fact the amphiphile concentrations in the water-rich corner are much lower than those in the oil-rich corner.

In summary, with nonionic amphiphiles, the three-phase body appears by separation of a water-rich micellar solution at T_l, being in equilibrium with a molecularly disperse oil-rich phase b. With rise in temperature, the number density of micelles in the water-rich phase (a) decreases, whereas the o/w dispersion in the amphiphile-rich phase (c) becomes more concentrated, both phases being in equilibrium with the molecularly disperse oil-rich phase (b) the amphiphile concentration in which increases. At a temperature near the mean temperature $\bar{T}$ of the three-phase temperature interval ΔT, the amphiphile concentrations in phase a and b reach the corresponding cmc's, those in phase a reaching cmc^a from above, those in phase b reaching cmc^b from below. All excess amphiphile is now concentrated in phase c, forming a spongelike structure of water and oil domains. With further rise in temperature, the number density of (inverse) micelles in phase b increases, whereas the sponge in phase c breaks up into a w/o dispersion, both phases being in equilibrium with the now molecularly disperse water-rich phase a, until at T_u the compositions of phases c and b become identical.

At temperatures below $\bar{T}$, the amphiphile concentration at the break of the slope in the $\sigma_{ab}/\log\gamma$ curve defines the cmc^a tie line as a function of α, whereas above $\bar{T}$ it defines the cmc^b tie line. At $\bar{T}$, the break coincides with the a–b side of the three-phase triangle. At temperatures below or above $\bar{T}$ but within ΔT, the break, therefore, lies at amphiphile concentrations below the a–b side, so that, when measuring σ_{ab} vs γ in the two-phase region approaching the a–b side, one finds the break before the third amphiphile-rich phase c appears. This can be readily demonstrated near the oil-rich corner at which the corresponding amphiphile concentrations are considerably higher than in the water-rich corner. Figure 17 shows a $\sigma_{ab}/\log\gamma$ curve in the $A-B_{10}-C_8E_3$ mixture, measured by means of a spinning drop apparatus at α = 80 wt % and 28.6 °C, that is, just below T_u. The break, defining cmc^b, lies at γ = 2.65 wt %, whereas the third phase appears at 5.5 wt %, defining the a–b tie line of the three-phase triangle at these particular values of T and α. Within the three-phase body, σ_{ab} was measured after careful removal of the middle phase.

XI. Solubilization along the Binodals

Figure 18 shows the straight portions of some binodals on the water-rich (left) and on the oil-rich side (right) for $A-B_8-C_{10}E_4$ mixtures, with T as parameter. The first information that can be obtained from this figure is the temperature dependence of cmc^b as shown on the right of Figure 14 for the $A-B_8-C_8E_4$ mixture. The second information is the temperature dependence of the initial slope of the binodals, that is, the angle between their straight

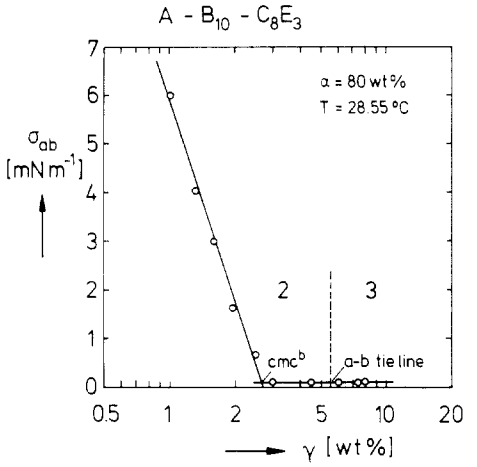

Figure 17. Interfacial tension σ_{ab} vs log γ in $A-B_{10}-C_8E_3$ in the oil-rich corner at $\bar{T} < T < T_u$, demonstrating the distance between the cmc^b tie line and the a–b side of the three-phase triangle.

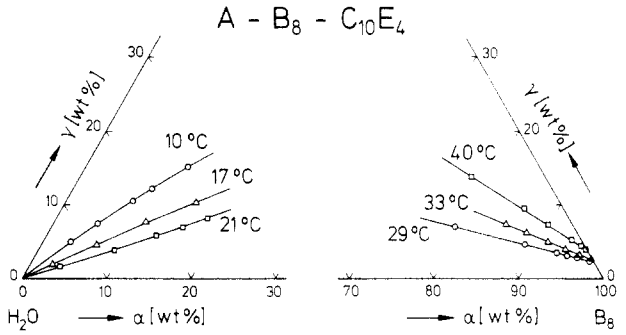

Figure 18. Temperature dependence of the straight portions of the binodals in the water-rich (left) and the oil-rich corner (right) in $A-B_8-C_{10}E_4$.

portions and A–C or B–C side, respectively, of the Gibbs triangle. As one can see, the slope on the water-rich side increases as one approaches $\bar{T}$ (≈25 °C) from below, whereas that on the oil-rich side increases as one approaches $\bar{T}$ from above. The slope of the binodals is a measure for the number k_i of solubilized solute molecules per amphiphile molecule, k_b standing for solubilized oil molecules in the o/w droplets on the water-rich side, k_a standing for water molecules in the w/o droplets on the oil-rich side. In view of eq VII.6, again if the thickness of the interfacial layer is neglected, k_i is given by

$$k_i = (1/3)(V_i\Gamma)^{-1}r \qquad \text{(XI.1)}$$

where V_i is the molar volume of solute i. Assuming Γ to depend only weakly on T in the considered temperature range, the temperature dependence of k_i should thus be that of r.

At constant T, σ_{ab} remains constant above the cmc surface up to rather high amphiphile concentrations before it eventually starts dropping to vanish at the plait point. Within that concentration range one may, therefore, set σ_{ab} equal to that at the cmc surface. In view of Figure 2, σ_{ab} can be approximated by a parabola with its minimum near $\bar{T}$

$$\sigma_{ab} = \sigma_0 + \Theta(T - \bar{T})^2 \qquad \text{(XI.2)}$$

where $\sigma_0 \equiv \sigma_{ab}(T = \bar{T})$. Inserted into (VII.3) this gives

$$r/r_0 = (T/\bar{T})^{1/2}\{1 + (\Theta/\sigma_0)(T - \bar{T})^2\}^{-1/2} \qquad \text{(XI.3)}$$

where $r_0 \equiv r(T = \bar{T})$. For a representative example we have set $\bar{T}$ = 300 K, $\sigma_0 = 1 \times 10^{-2}$ mN m^{-1}, and $\Theta = 1 \times 10^{-3}$ mN m^{-1} K^{-2}. Figure 19 shows on its left the temperature dependence of σ_{ab}, and on its right that of r/r_0. This result predicts that the radii of the o/w droplets along the straight portion of the binodal on the water-rich side at $T = \bar{T} - \Delta$ should be equal to those of the w/o droplets along the binodal on the oil-rich side at $T = \bar{T} + \Delta$. If combined with eq XI.1, it furthermore predicts that k_b should

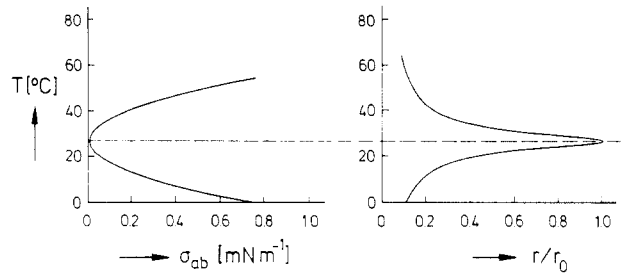

Figure 19. Relation between interfacial tension σ_{ab} and radius r of droplets after eq XI.3.

increase as one approaches $\bar{T}$ from below, whereas k_a should increase as one approaches $\bar{T}$ from above, in qualitative agreement with Figure 18.

The number k_i of solubilized solute molecules per amphiphile molecule, that is, the slope of the two binodals, differ, of course. The ratio between k_b on the water-rich side at $T = \bar{T} - \Delta$ and k_a on the oil-rich side at $T = \bar{T} + \Delta$ is given by eq XI.1, that is, by the ratio of the molar volumes

$$k_b(\bar{T} - \Delta)/k_a(\bar{T} + \Delta) = V_A/V_B \approx 1/10 \qquad \text{(XI.4)}$$

which agrees well with the ratios found by Aveyard and coworkers[26] in $A-B_k-C_{12}E_5$ mixtures.

For estimating k_a near $\bar{T}$, that is, near its maximum, one may set again in eq VII.3 and XI.1, respectively, $\sigma_{ab} = 1 \times 10^{-2}$ mN m^{-1}, $k_BT = 4 \times 10^{-14}$ erg, and $\Gamma = 3 \times 10^{-10}$ mol cm^{-2}, to find with $V_A = 18$ cm^3 mol^{-1} about 120 water molecules per amphiphile molecule which is of the correct order of magnitude. Because the thickness of the interfacial layer has been neglected in this estimate, the actual number should be somewhat smaller, the error increasing with increasing σ_{ab}, that is, decreasing r.

XII. The Trajectories of the Critical Lines

As can be seen in Figure 16, both phase a and cmc^a move toward the A corner with rising temperature, phase a overtaking cmc^a near $\bar{T}$. On the oil-rich side one finds the inverse: both phase b and cmc^b move toward the B corner with dropping temperature, phase b overtaking cmc^b at the same temperature near $\bar{T}$. The rapid movement of phases b and a originates in the trajectories of the two critical lines cl_α and cl_β, respectively, that enter the phase prism at the critical points cp_α and cp_β, and terminate at the corresponding critical end points cep_α and cep_β. While in mixtures with short-chain amphiphiles both critical lines proceed monotonically into the phase prism before terminating at their corresponding end points, in mixtures with medium- and long-chain (nonionic) amphiphiles, they overshoot the critical end points; that is, cl_α on the oil-rich side ascends very steeply and passes through a maximum at a temperature above T_u before it approaches cep_α from above. On the water-rich side, cl_β descends rather steeply and passes through a minimum at a temperature below T_l before it approaches cep_β from below. This was first observed by Shinoda and Saito in 1968.[27] Figure 20 shows on top vertical sections through the phase prism of the $A-B_8-C_{10}E_4$ mixture, the one on the left erected in the water-rich corner, the one on the right in the oil-rich corner. The curve through the empty circles on the upper left, although not being identical with the critical line cl_β, resembles the trajectory of cl_β. The curve through the empty squares on the upper right, although not being identical with cl_α, resembles the trajectory of the latter. Both overshoot their end points. As one approaches the central miscibility gap from the oil-free side at a temperature just below T_l, the micellar solution thus first separates at a plait point lying on the descending part of cl_β, becomes homogeneous again at a plait point on the ascending part of cl_β, before it finally, separates into phases a and b. On the oil-rich side one finds the inverse: as one approaches the central gap from the water-free side at a temperature just above T_u, the (inverse) micellar solution first separates at a plait

(26) Aveyard, R.; Binks, B. P.; Fletcher, P. D. I. *Langmuir* **1989**, *5*, 1210.
(27) Shinoda, K.; Saito, H. *J. Colloid Interface Sci.* **1968**, *26*, 70.

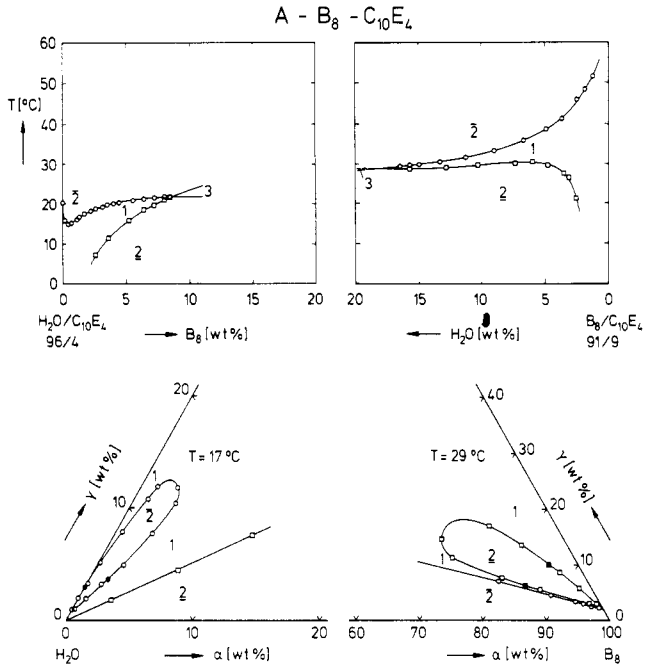

Figure 20. (Top) Vertical sections through the A–B_8–$C_{10}E_4$ prism on the water-rich (left) and oil-rich side (right), demonstrating the trajectories of the corresponding critical lines cl_β and cl_α, respectively. (Bottom) Two-phase loops separated from the central miscibility gap at $T < T_l$ (left), and $T > T_u$ (right). The full points represent experimentally determined plait points.

point lying on the ascending part of cl_α and becomes homogeneous again at a plait point on the descending part of cl_α before it finally separates into phases b and a. As a consequence, isothermal sections through the phase prism at temperatures just below T_l or just above T_u, respectively, show the central miscibility gap with isothermal loops on each side (Figure 20, bottom), the tie lines of which run essentially parallel to the A–C or B–C side, respectively, of the Gibbs triangle as can be deduced from the loci of the (full) plait points.

As one raises the temperature (on the water-rich side), the oil-rich plait point of the loop approaches the central miscibility gap to touch it a T_l which leads to the separation into phases a and c. Because the tie lines of the loop run essentially perpendicular to those of the central miscibility gap, the two phases move rapidly apart with further rising temperature, phase a, in particular, overtaking cmc[a] near $\bar{T}$ (Figure 16). On the oil-rich side one finds the inverse: as one drops temperature, the water-rich plait point of the loop approaches the central gap to touch it at T_u which leads to the separation into phases b and c. With further drop in temperature, phase b moves rapidly toward the B corner to overtake cmc[b].

The reason why micellar solutions at temperatures just below T_l or above T_u first separate into two coexisting phases with increasing concentration of the solute (either oil or water) and become homogeneous again with further increasing solute concentration before they, finally, expel the solute as second bulk phase has still to be clarified. This feature is, apparently, related to the transition from weakly structured solutions to microemulsions. Experiment shows that the critical lines cl_β in A–B_8–C_iE_j mixtures with C_4E_1 and C_6E_3 descend monotonically to their critical end points on the water-rich side, whereas that with C_8E_4 is the first in this series to overshoot its cep. For medium- and long-chain nonionic amphiphiles, the critical line cl_β on the water-rich side thus appears as bicritical point at a temperature below T_l. With rising temperature, this point develops into a loop (Figure 20, lower left), the oil-rich plait point of which touches the central miscibility gap as critical end point cep_β at $T = T_l$. The critical line cl_α on the oil-rich side, on the other hand, appears as bicritical point at a temperature above T_u. With dropping temperature, this point develops into a loop (Figure 20, lower right), the water-rich plait point of which touches the central miscibility gap as critical end point cep_α at $T = T_u$.

XIII. Conclusion

The phase behavior of mixtures composed of water, a nonpolar solvent, and an amphiphile is determined by the interplay of the miscibility gaps in the corresponding binary mixtures. So far, the phase behavior of microemulsion does not differ from that of other ternary mixtures, in particular, of mixtures with short-chain amphiphiles. This holds, in particular, for the separation of such mixtures into three coexisting liquid phases within a well-defined temperature interval ΔT. While mixtures with short-chain amphiphiles are weakly structured, those with medium- and long-chain amphiphiles may form stable colloidal dispersions of o/w or w/o domains with diameters of the order of 10 nm. This is made possible by the very low interfacial tension σ_{ab} between the water-rich and the oil-rich phases due to the adsorption of amphiphiles at that interface, being a consequence of the opposite interaction energies between amphiphiles and water or nonpolar solvents, respectively. As a consequence, there exist two cmc surfaces spanning from the water-rich or the oil-rich mixture through the body of heterogeneous phases to the opposite side of the binodal surface, the competition between which determines which of the solvents is dispersed by the excess amphiphile. The tendency for forming micelles, and thus for forming large domains, increases gradually with increasing amphiphilicity, so that the evolution from weakly structured mixtures to microemulsions is gradual. It is, therefore, suggested that microemulsions be defined as stable colloidal dispersions with domains sufficiently large for the dispersed solvent to exhibit the properties of a bulk phase. Because the interfacial tension σ_{ab} reaches a minimum at the mean temperature $\bar{T}$ of the three-phase temperature interval, microemulsions in this narrower sense are most likely to be found near $\bar{T}$ at amphiphile concentrations close to the binodal surface. For drawing the borderline between weakly structured mixtures and microemulsions experimentally, one may, e.g., study the kinetics of chemical reactions in w/o dispersions that permit determining the effective relative dielectric permittivity (dielectric number) in the water domains as it depends on the domain size. Such studies are in progress.[28]

With respect to the currently discussed theories of microemulsions, one has to distinguish between two approaches. In the first one the mixture is considered as a lattice with a molecule of one of the three components on each site. Such a model was first studied by Wheeler and Widom[29] in 1968. The authors considered "difunctional" molecules of the type A–A, B–B, and A–B, assuming that contacts of A ends with A ends, and of B ends with B ends, are favored over contacts of A ends with B ends. The lattice approach was developed further by Widom, Dawson, Wheeler, and Schick.[30] The second one is a phenomenological description, based on a paper by Talmon and Prager,[31] and further developed by De Gennes et al., Widom, and Safran et al.[32] It considers the ternary mixture as an essentially binary mixture of water and oil domains with the amphiphilic monolayer being treated as a flexible membrane with a bending energy that contributes to the excess free energy. The theory predicts the interfacial tension σ_{ab} of a plane interface to be proportional to the square of a "natural curvature" c_0, and the "preferred" droplet radius to scale as c_0^{-1}, which is in qualitative agreement with eq VII.3. It is beyond the scope of this review to compare the predictions of the various models with experiment. Most of them yield three-phase triangles with a spongelike structure of the middle phase, as well as lyotropic mesophases at higher amphiphile concentrations. What remains to be done is to clarify the relation between the parameters appearing in the free energy equations and the characteristic properties of the phase diagrams of the

(28) Schomäcker, R., to be published.
(29) Wheeler, J. C.; Widom, B. *J. Am. Chem. Soc.* **1968**, *90*, 3064.
(30) For a review see, e.g.: Gompper, G.; Schick, M. In *Modern Ideas and Problems in Amphiphilic Science*; Gelbart, W. M., Roux, D., Ben-Shaul, A., Eds.; to be published.
(31) Talmon, Y.; Prager, S. *J. Chem. Phys.* **1978**, *69*, 2984.
(32) For a review see, e.g.: Safran, S. A., to be published in ref 30.

binary mixtures including the cmc's. Most needed, however, is clarification of the nature of the various microstructures in water-amphiphile mixtures because many features of the ternary mixtures are apparently already present in the oil-free mixtures and are merely amplified by adding oil.

Acknowledgment. M.K. is indebted to Dr. H. Reiss for stimulating discussions during a visit to the UCLA. We, furthermore, acknowledge valuable contributions by Dr. D. Haase, Dr. R. Schomäcker, and K. V. Schubert. Last, but not least, we are indebted to J. Da Corte, A. Ellroth, B. Faulhaber, T. Lieu, and Th. Sottmann for their assistance with the experiments, and to D. Luckmann for drawing the figures. The work was in part supported by the German Ministry for Research and Technology (BMFT) (Grant No. 0326315 B), and by a NATO travel grant (No. O425/88).

ARTICLES

Intramolecular Charge Transfer in Donor-Acceptor Molecules

A. Slama-Schwok, M. Blanchard-Desce, and J.-M. Lehn*

Chimie des Interactions Moléculaires, Collège de France, 11 Place Marcelin Berthelot, 75005 Paris, France
(Received: June 7, 1989; In Final Form: November 9, 1989)

The photophysical properties of donor-acceptor molecules, "push-pull" polyenes and carotenoids, have been studied by absorption and fluorescence spectroscopy. The compounds bear various acceptor and donor groups, linked together by chains of different length and structure. The position of the absorption and fluorescence maxima and their variation in solvents of increasing polarity are in agreement with long-distance intramolecular charge-transfer processes, the linker acting as a molecular wire. The effects of the linker length and structure and of the nature of acceptor and donor are presented.

Introduction

Modification and functionalization of natural carotenoids[1] is an efficient way for molecular engineering of polyenic chains, yielding synthetic molecules of interest in the field of molecular electronics.[2,3] Symmetrically substituted bipyridinium carotenoids, the caroviologens, represent a molecular wire approach to electronic conduction.[3] Unsymmetrical substituted polyene chains bearing an anthryl group at one end and a tetraphenylporphyrin group at the other end display energy transfer between the two terminal units.[4] The anchoring of a carotenoid chain to a porphyrin linked to a quinone group leads to biomimetic systems, of triad type, that undergo long-lived photodriven charge separation, of potential value for photochemical energy storage.[5] On the other hand, very fast charge-transfer processes are of interest as potential molecular devices, for long-distance signal processing and transfer.[6] This may be achieved by "push-pull" carotenoids, obtained by anchoring of the electron donor and acceptor at the opposite terminal ends of the polyenic chain.[7] These compounds should present interesting photophysical properties and undergo (partial) intramolecular charge transfer upon excitation. Such phenomena have been observed in a number of donor-acceptor conjugated molecules like push-pull benzenes (with *p*-nitroaniline as a prototype),[8,9] stilbenes,[9,10] biphenyls,[9,11,12] polyphenyls,[9] and more

CHART I

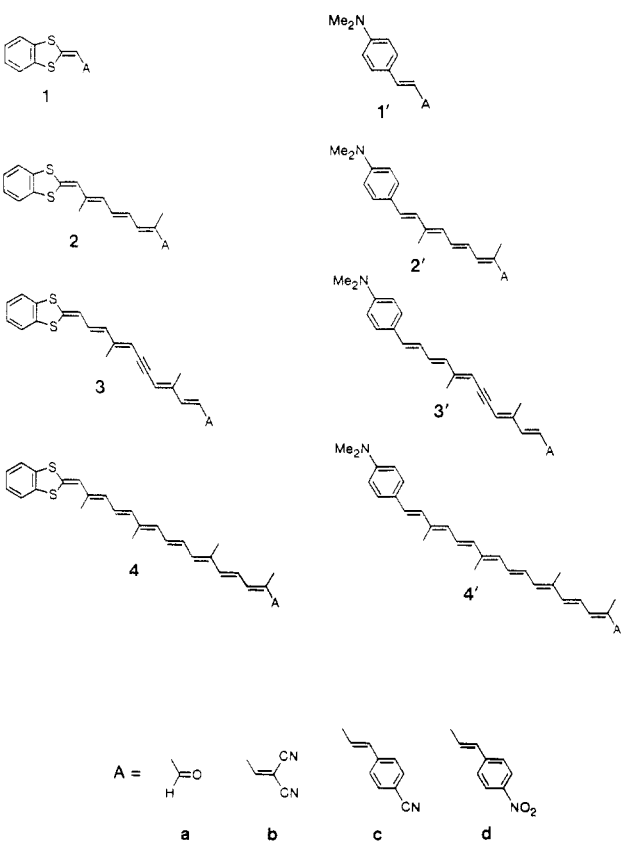

(1) *Carotenoids*; Isler, O., Ed.; Birkhäuser Verlag: Basel, Switzerland, 1971.
(2) (a) Haddon, R. C.; Lamola, A. A. *Proc. Natl. Acad. Sci. U.S.A.* **1985**, *82*, 1874. (b) Munn, R. W. *Chem. Br.* **1984**, 518.
(3) Arrhenius, T. S.; Blanchard-Desce, M.; Dvolaïtzky, M.; Lehn, J.-M.; Malthête, J. *Proc. Natl. Acad. Sci. U.S.A.* **1986**, *83*, 5355.
(4) Effenberger, F.; Schlosser, M.; Bäukerle, P.; Maier, S.; Port, H.; Wolf, H. C. *Angew. Chem., Int. Ed. Engl.* **1988**, *27*, 281.
(5) (a) Moore, T. A.; Gust, D.; Mathis, P.; Mialocq, J. C.; Chachaty, C.; Bensasson, R. V.; Land, E. J.; Doizi, D.; Liddell, P. A.; Nemeth, G. A.; Moore, A. L. *Nature* **1984**, *307*, 630. (b) Seta, P.; Bienvenue, E.; Moore, A. L.; Mathis, P.; Bensasson, R. V.; Liddell, P.; Pessiki, P. J.; Joy, A.; Moore, T. A.; Gust, D. *Nature* **1985**, *316*, 653. (c) Gust, D.; Moore, T. A.; Moore, A. L.; Barrett, A.; Harding, L. O.; Makings, L. R.; Lidell, P. A.; De Schryver, F. C.; Van der Auweraer, M.; Bensasson, R. F.; Rougée, M. *J. Am. Chem. Soc.* **1988**, *110*, 321.
(6) Lehn, J.-M. *Angew. Chem., Int. Ed. Engl.* **1988**, *27*, 107.
(7) Blanchard-Desce, M.; Ledoux, I.; Lehn, J.-M.; Malthête, J.; Zyss, J. *J. Chem. Soc., Chem. Commun.* **1988**, 736.

0022-3654/90/2094-3894$02.50/0